Progress in Oceanography 162 (2018) 160–170

Contents lists available at ScienceDirect

Progress in Oceanography

journal homepage: www.elsevier.com/locate/pocean

Long-term patterns of benthic irradiance and kelp production in the central Beaufort sea reveal implications of warming for Arctic inner shelves

Christina Bonsell*, Kenneth H. Dunton

University of Texas Marine Science Institute, 750 Channel View Dr., Port Aransas, TX 78373, USA

ARTICLE INFO

Keywords:
Arctic zone
Kelp
Coastal zone
Long-term records
Light attenuation
Sea ice

ABSTRACT

This study synthesizes a multidecadal dataset of annual growth of the Arctic endemic kelp *Laminaria solidungula* and corresponding measurements of *in situ* benthic irradiance from Stefansson Sound in the central Beaufort Sea. We incorporate long-term data on sea ice concentration (National Sea Ice Data Center) and wind (National Weather Service) to assess how ice extent and summer wind dynamics affect the benthic light environment and annual kelp production. We find evidence of significant changes in sea ice extent in Stefansson Sound, with an extension of the ice-free season by approximately 17 days since 1979. Although kelp elongation at 5–7 m depths varies significantly among sites and years (3.8–49.8 cm yr^{-1}), there is no evidence for increased production with either earlier ice break-up or a longer summer ice-free period. This is explained by very low light transmittance to the benthos during the summer season (mean daily percent surface irradiance ± SD: 1.7 ± 3.6 to 4.5 ± 6.6, depending on depth, with light attenuation values ranging from 0.5 to 0.8 m^{-1}), resulting in minimal potential for kelp production on most days. Additionally, on month-long timescales (35 days) in the ice-free summer, benthic light levels are negatively related to wind speed. The frequent, wind-driven resuspension of sediments following ice break-up significantly reduce light to the seabed, effectively nullifying the benefits of an increased ice-free season on annual kelp growth. Instead, benthic light and primary production may depend substantially on the 1–3 week period surrounding ice break-up when intermediate sea ice concentrations reduce wind-driven sediment resuspension. These results suggest that both benthic and water column primary production along the inner shelf of Arctic marginal seas may decrease, not increase, with reductions in sea ice extent.

1. Introduction

Seasonal sea ice cover plays a prominent role in marine primary productivity in high-latitude ecosystems, as it can set the timing of peak production and determine annual light budgets (Kahru et al., 2011; Clark et al., 2013; Ji et al., 2013; Post et al., 2013). In the Arctic Ocean, there has been a striking decline in sea ice extent since the onset of observations via satellite measurements, at a rate of approximately 13.3% loss in area per decade (Serreze and Stroeve, 2015). Despite ongoing efforts by scientists to investigate the effects of sea ice loss on pelagic production (reviewed in Wassmann and Reigstad, 2011), only a few studies to date have addressed the direct consequences on benthic production (Krause-Jensen et al., 2012; Clark et al., 2013; Krause-Jensen and Duarte, 2014). In coastal Arctic systems, benthic primary production by macro- and micro-algae in Arctic waters is important to ecosystem production, elemental cycling, and food web dynamics, especially during times of limited pelagic production (Dunton and Schell, 1987; Glud et al., 2009; McMeans et al., 2015; Renaud et al., 2015). Additionally, bio-physical processes in shallow, nearshore Arctic areas, where much of this production takes place, remain understudied due to logistical constraints (e.g. Fritz et al., 2017). Changes to production in these areas would have broad consequences for Arctic ecosystem function.

Because of the strong annual cycle of solar irradiance in polar regions, seasonal sea ice and solar energy models predict that earlier dates of ice break-up will result in exponential increases in benthic light budgets (Clark et al., 2013). For instance, Krause-Jensen et al. (2012) and Clark et al. (2013) used existing gradients in seasonal ice cover in Greenland and Antarctica, respectively, to link lengthened ice-free seasons with increases in macroalgal production and hypothesized that future warming-driven reductions in seasonal sea ice extent and duration will enhance annual production by benthic macrophytes. These predictions contribute to the idea that Arctic coastal habitats will become increasingly macrophyte-dominated as Arctic warming continues, with consequences for Arctic food webs and seawater chemistry (Clark et al., 2013; Krause-Jensen and Duarte, 2014; Krause-Jensen et al.,

* Corresponding author.
E-mail addresses: cbonsell@utexas.edu (C. Bonsell), ken.dunton@utexas.edu (K.H. Dunton).

https://doi.org/10.1016/j.pocean.2018.02.016
Received 6 July 2017; Received in revised form 15 February 2018; Accepted 17 February 2018
Available online 19 February 2018
0079-6611/

2016). However, variations in underwater optical properties, which have a profound influence on light transmittance to the benthos and demonstrable impacts on benthic primary production (Van Duin et al., 2001), are largely overlooked in these analyses. Bartsch et al. (2016) hypothesized that enhanced sediment inputs from glacial melt caused a narrower euphotic zone during the open-water season, leading to observed shallowing of peak biomass and shallower depth limit of kelps in Svalbard over the past two decades. The links between ice loss, irradiance at depth, and primary production appear to be multifaceted and warrant further investigation.

While ice cover determines irradiance at the water's surface, irradiance at depth depends on light attenuation in the water column. In the coastal Arctic Ocean, summer water transparency is influenced by concentrations of phytoplankton and sediments suspended in the water column. Concentrations of suspended sediments during the open-water summer in the coastal Beaufort Sea have been directly linked to increased light attenuation and decreased annual production by benthic macroalgae (Aumack et al., 2007). Many Arctic inner shelf areas (depth < 10 m), such as the Alaskan Beaufort Sea coast, have particularly high suspended sediment concentrations due to shallow depth, persistence of unconsolidated sediments, and significant inputs by numerous rivers and streams (notably, the Arctic Ocean receives 11% of global river discharge, but only constitutes 1% of global ocean volume; McClelland et al., 2011). These sediments originate from coastal erosion, resuspension due to water motion, and fluvial inputs by Arctic rivers, which discharge the large majority of their annual suspended sediment loads by the end of the spring melt (Wegner et al., 2003; O'Brien et al., 2006; Walker et al., 2008). Because most river fluxes occur before the end of ice break-up, changes in wind direction and/or speed during the open-water period are the main drivers of temporal variability in underwater irradiance in the nearshore areas, as they are in other shallow aquatic systems (Van Duin et al., 2001). Annual benthic light budgets may consequently have a negative relationship with wind speeds during the ice-free season.

The primary objective of this paper is to examine how sea ice extent and wind dynamics affect variation in the annual benthic light budget and production by the Arctic endemic kelp *Laminaria solidungula* in the central Beaufort Sea. Since 1979, sea ice duration in the Beaufort Sea has decreased at an accelerating rate, while summertime easterly winds have increased in speed and frequency across the coastal region (Wood et al., 2013, 2015; Frey et al., 2015). These long-term environmental changes may have significant, but opposing, effects on long-term primary production patterns. Although lengthened ice-free season results in increased irradiance at the waters' surface, enhanced summer winds may degrade the underwater light climate. Frond elongation in *L. solidungula*, is entirely dependent on the utilization of photosynthetically derived carbon reserves produced the previous summer (Dunton and Schell, 1986). The resulting annual growth has a strong correlation with the light budget of the preceding ice-free season (Dunton, 1990). This species is ideal for assessing the biological effects of changes to the Arctic underwater light environment due to its enhanced capacity to respond to small changes in irradiance compared to other kelp species, particularly evident in its low saturating irradiance for photosynthesis (38 µmol photons sec^{-1}; Dunton and Jodwalis, 1988).

Multidecadal time series that document biological responses to variations in regional climate in Arctic marine systems are rare, but critical for the development of accurate projections of future ecosystem change (Wassmann et al., 2011). Here, we synthesize a multidecadal dataset (collected between 1977 and 1992, and 2002 through 2008) and incorporate previously unpublished data (2012 through 2016), on benthic irradiance and kelp growth from Stefansson Sound in the central Beaufort Sea (Dunton, 1990; Dunton et al., 1992, 2009; Aumack et al., 2007) to demonstrate the combined influence of seasonal ice extent and wind dynamics on the annual light budget, and annual kelp production. Additionally, we assess whether annual variations in *L. solidungula* growth relate to seasonal ice extent and summer wind dynamics. In doing so, this work highlights the importance of including factors that affect underwater light transmittance in projecting changes in primary productivity and ecosystem structure in Arctic marine ecosystems.

2. Methods

2.1. Study site

The Stefansson Sound Boulder Patch (hereafter 'the Boulder Patch') is an isolated rocky zone of boulders and cobbles covering an area of approximately 63 km^2 in a region dominated by soft sediment (Barnes and Reimnitz, 1974; Fig. 1). Located in relatively shallow water (4–8 m) within 15 km of the coast, the Boulder Patch remains a non-depositional environment despite its proximity to the Sagavanirktok River, which has a 1–2 week period of peak discharge in late May and early June (Dunton et al., 1982; Rember and Trefry, 2004)

The epilithic community in the Boulder Patch is dominated by the kelp *L. solidungula* and represents a regional biodiversity hotspot. Research conducted in the area since the 1970s has focused primarily on characterizing the underwater light environment and the biological production of *L. solidungula* (Dunton, 1985; Dunton and Schell, 1986, 1987, Dunton et al., 1992, 2009; Henley and Dunton, 1995; Aumack et al., 2007). Field studies have been nearly continuous since 1978 except for a single seven-year lapse (1993–2000), with ten long-term study sites occupied since 1984 (Fig. 1).

2.2. Kelp production

Laminaria solidungula individuals from long-term study sites were collected by SCUBA divers at one- or two-year intervals. The thallus of this species consists of a single blade with multiple ovate growth sections, each representing one year of production. The blade section closest to the stipe represents production from the most recent year and the immediate distal section represents growth from the previous year. Because multiple years of production can be measured from a single individual, this dataset spans from 1976 to 1990 and 1996 to 2015.

2.3. Benthic and surface irradiance

Spherical quantum sensors (LI-193SA, LI-COR Inc.), placed ~0.5 m above the benthos, were deployed for measurements of photosynthetically active radiation (PAR) at sites across the Boulder Patch (Fig. 1, Supp. Table 1). Sensors were deployed in conjunction with either CR21 (Campbell Scientific), LI-1000, LI-1400, or LI-1500 dataloggers (LI-COR Inc.), depending on the site and study year (Supp. Table 1). Cosine PAR sensors (LI-192SA, LI-COR Inc.) deployed in line with a LI-1000 datalogger collected continuous surface light measurements at East Dock in Prudhoe Bay (1986–1987) and Endicott Island (1987–2016; Fig. 1). Sensors were cleaned between deployments (once a year), as bio-fouling in this environment is negligible. Sensors made instantaneous measurements every minute and logged the average every 1 or 3 h, depending on site and study year (Supp. Table 1). All PAR measurements were converted into total daily photon flux rate (mol m^{-2} day^{-1}) for analysis. Daily hours of saturating irradiance for *L. solidungula* (H_{sat}: hours with average photon flux rate ≥ 38 µmol photon m^{-2} sec^{-1}; Dunton and Jodwalis, 1988) were also calculated, as this metric is more closely related to annual production than photon flux rate (Dunton, 1990). For years with irradiance data for > 90% of the year, annual H_{sat} was calculated at each site.

2.4. Sea ice

Sea ice concentration from 1979 to 2016, measured via passive microwave data, was obtained from the National Sea Ice Data Center via the Arctic Data Integration Portal (http://portal.aoos.org) for the

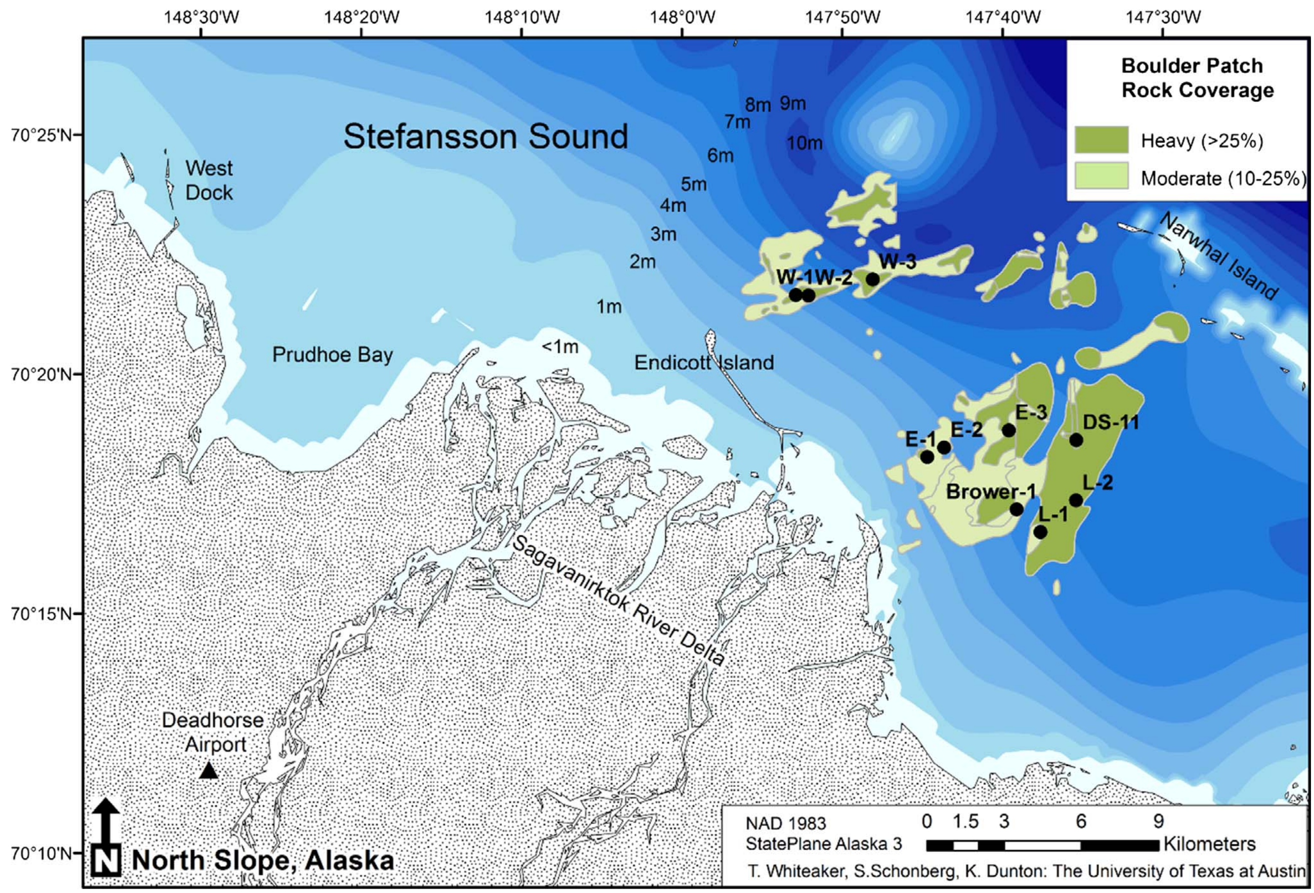

Fig. 1. The Stefansson Sound Boulder Patch, showing location of long-term study sites in relation to percent rock cover in Stefansson Sound. Inset shows location of Stefansson Sound (blue star) in reference to Alaska. (For interpretation of the references to colour in this figure legend, the reader is referred to the web version of this article.)

two 25 km^2 grid areas that contain the Boulder Patch. Values from the two areas mirrored each other closely over time and were therefore averaged daily. Dates of key events in the ice season (break-up start, break-up end, freeze-up start, and freeze-up end) were calculated using the algorithms described by Johnson and Eicken (2016). These events define the seasonality of direct incident solar radiation to the sea surface. The length of the ice-free season was calculated as freeze-up start minus break-up end.

2.5. Wind

Wind speed and direction for West Dock in western Stefansson Sound (National Climate Data Center ID 9497645), spanning 1993–2016, were obtained from the National Weather Service Cooperative Observer Program (COOP) via the R package "r-noaa" (Chamberlain, 2016). Wind speed and direction for Deadhorse Airport, spanning 1973–2016, were obtained from the Alaska Airport Weather Observations Network (mesonet.agron.iastate.edu/ASOS/) and underwent quality control procedures before analysis. Coastal wind speed was estimated from the Deadhorse data using the linear relationship between wind speed at Deadhorse and West Dock (see *Results*). For consistency, we only used the estimated coastal wind speed in analyses relating to irradiance and kelp growth. To examine changes in summer winds over time, we used data confined by the dates of start of break-up and start of freeze-up for each year; for analyses relating wind to benthic light or kelp growth, we focused on wind data confined by the dates of end of break-up and start of freeze-up for each year. In concurrence with other studies in the region, storm events were defined as > 6 consecutive hours of average wind speeds over 10 m/s, with direction defined by primary cardinal direction (e.g. winds from NNE were defined as N winds; Manson and Solomon, 2007).

To assess the effect of wind speed on underwater light transmittance, we plotted the relationship between mean daily coastal wind speed (as estimated from Deadhorse) and daily percent surface irradiance. Due to noisy data, wind speeds were binned by rounding to the nearest whole number.

2.6. Production model

To assess the effects of ice extent and wind speed on annual kelp production, we used the model developed by Aumack et al. (2007) to calculate daily production rates under given depth and suspended sediment concentrations. Briefly, this model uses incident radiation and a suspended sediment concentration-specific light attenuation coefficient to estimate benthic irradiance to calculate *L. solidungula* production over the open-water season. We estimated incident radiation on each day of the year by averaging values for each day from all the years of surface irradiance measurements. We incorporated daily wind speeds by using estimates of suspended sediment concentrations under given wind speeds obtained in this region (Trefry et al., 2009, Aumack and Dunton *unpublished data*; Supp. Table 2). We confined the model to ice-free dates only and used daily average coastal wind speed. Annual carbon production was estimated for the average size of individuals from our long-term dataset (22.5 cm basal blade length). Modelled carbon production was compared to the long-term kelp growth dataset, with measured kelp growth converted into g C yr^{-1} based on previously derived relationships (Dunton and Jodwalis, 1988; Aumack, 2003).

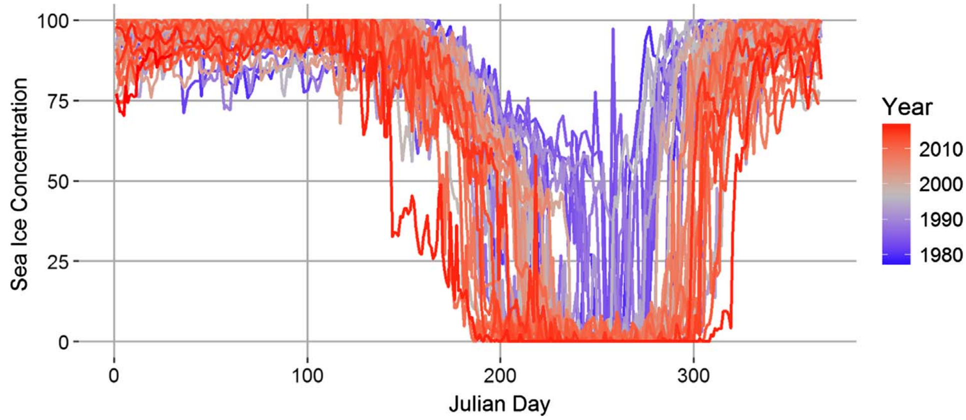

Fig. 2. Sea ice concentration by Julian Day in Stefansson Sound over a 38-year period (January 1979–2017) illustrates the lengthening of the open-water season and the decrease in summer ice concentration over time.

2.7. Statistical analysis

Trends in ice events, wind speed, and kelp growth over time were assessed using linear regression analyses. The relative effects of year and site, and the interaction between the two terms, on kelp growth were determined using ANOVA. We tested the relationships between kelp growth (linear elongation in centimeters) and date of ice break-up and length of ice free season by linear regression.

For years and sites with irradiance data for > 90% of the summer period (July-September), we tested if ice break-up date and length of ice-free season predicted the annual benthic irradiance budget using linear models. For these data, cumulative H_{sat} was calculated for each day by inclusively summing H_{sat} from all previous days to determine the seasonality of potential kelp production.

For all years of irradiance data, the longest portion of the year with representative data for multiple sites and years from multiple decades is 27 July – 31 August. There were not adequate redundancies in sites across years for these dates, so separate one-way ANOVAs were conducted to test the individual effects of site and year on three irradiance variables: (a) total annual irradiance, (b) mean irradiance, and (c) total H_{sat}. The relative effects of mean daily sea ice concentration and mean daily maximum wind speed, and the interaction between the two terms, on the three irradiance variables for this 36-day period were determined by linear regressions. As westerly winds entrain turbid coastal water in the nearshore in this region, we also tested the effects of wind direction and proportion of westerly winds on the three irradiance variables using linear regression. We defined westerly wind as within 45° of due west (270°). To test the relative importance of this period of time to annual kelp production, the relationships between site-specific annual kelp growth and total irradiance, as well as between site-specific annual kelp growth and total H_{sat}, were each tested by linear regression.

All analyses were carried out using R (R Core Team, 2016). Directional data was analyzed and plotted using the R package “circular” (Agostinelli and Lund, 2017).

3. Results

3.1. Physical drivers: sea ice and winds

We found that the ice-free season in Stefansson Sound (end of break-up to start of freeze-up) lengthened during the period of this study. Dates between ice break-up and freeze-up increased from 74 days in 1979 to 132 days in 2016 (Figs. 2 and 3, Supp. Table 3). Duration of ice break-up, however, did not show any change (Fig. 3, Supp. Table 3).

Coastal wind speeds directly measured at West Dock and estimated

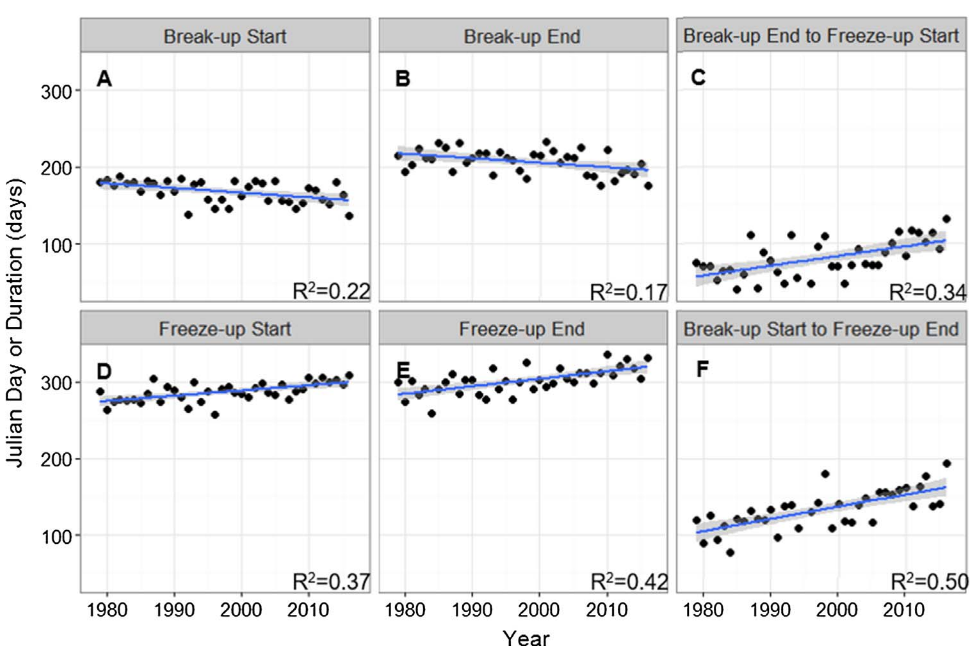

Fig. 3. Key events related to freeze-up and break-up by Julian Day (A-B,D-E) or duration of event in days (C,F). Generally, break-up is occurring earlier and freeze-up later over the 38-year period. Blue line represents the linear relationship ± SE (grey shading). (For interpretation of the references to colour in this figure legend, the reader is referred to the web version of this article.)

from Deadhorse show no trends over time (linear regressions on daily summer wind speed and fraction of hours with wind speeds > 10 m/s, $p > 0.05$, $R^2 < 0.1$). We also did not find evidence for a strengthening of easterly or westerly winds over time (linear regressions, $p > 0.05$, $R^2 < 0.1$). From the 1993–2016 data, we calculated the linear relationship between West Dock and Deadhorse daily wind speeds as

$$Speed_{West\ Dock} = 1.40 + 1.04*Speed_{Deadhorse} \quad (1)$$

where speeds are in m/s (linear regression, $p < 0.05$, $R^2 = 0.63$). Wind direction data for both stations are not vonMises distributed and therefore could not be analyzed statistically for trends over time. We discerned that mean wind direction at each station varies between years (particularly at Deadhorse), but typically originates from the east at West Dock and from the northeast at Deadhorse (Fig. 4).

3.2. In situ kelp growth and benthic irradiance: relationships to sea ice and wind

Analysis of the long-term data shows that kelp growth (as measured by blade elongation) in the Boulder Patch fluctuates over time and between sites (Fig. 5), although there is more variation in growth between sites than between years ($SS_{Site} = 80127$, $F_{Site}(98936) = 105$, $p < 0.01$ $SS_{Year} = 442890$, $F_{Year}(34,8936) = 153$, $p < 0.01$). The relationship between annual kelp growth across the Boulder Patch and the length of the open-water season is not significant (linear regression, $p > 0.05$, $R^2 < 0.1$).

Benthic irradiance at all sites displays strong seasonality, with some variation in maximum daily photon flux per year (Fig. 6). We only have data for the entire summer for a couple of years, confined mostly to the late 1980s and early 1990s, but we did not find any trends over time in the annual maximum daily photon flux rate (linear regressions performed for each site, $p > 0.05$, $R^2 < 0.1$). Under ice cover, no measurable light occurs except at some sites in some years in the spring under "clean ice" (Dunton, 1984), until around the time of the freshet when irradiance levels return to zero (Fig. 6). The first significant light transmittance occurs after ice break-up has begun (Figs. 6 and 7). Overall summer light levels are low, with the majority of days lacking light levels that approach saturation irradiance for *Laminaria solidungula* (Table 1). Interestingly, these data show that the days surrounding ice break-up contribute strongly to annual H_{sat} for a given site, sometimes over 50% of the annual value (Fig. 7).

Our analysis of data from 27 July – 31 August showed no significant differences among sites for mean daily benthic irradiance (MDI), total benthic irradiance (TBI), or total H_{sat} (TH). However, we detected significant differences among years for this period ($SS_{MDI\sim Year} = 10.58$, $F_{MDI\sim Year}(6,18) = 9.95$, $p < 0.01$; $SS_{TBI\sim Year} = 12102$, $F_{TBI\sim Year}(6,18) = 10.54$, $p < 0.01$; $SS_{TH\sim Year} = 85591$, $F_{TH\sim Year}(6,18) = 11.8$, $p < 0.01$). TBI and TH from this period do not predict annual kelp growth (linear regressions, $p > 0.05$, $R^2 < 0.1$). We did not find significant effects of mean daily sea ice concentration, or the interaction between ice concentration and mean daily maximum wind speed on MDI, TBI, or TH. However, mean daily maximum wind speed alone

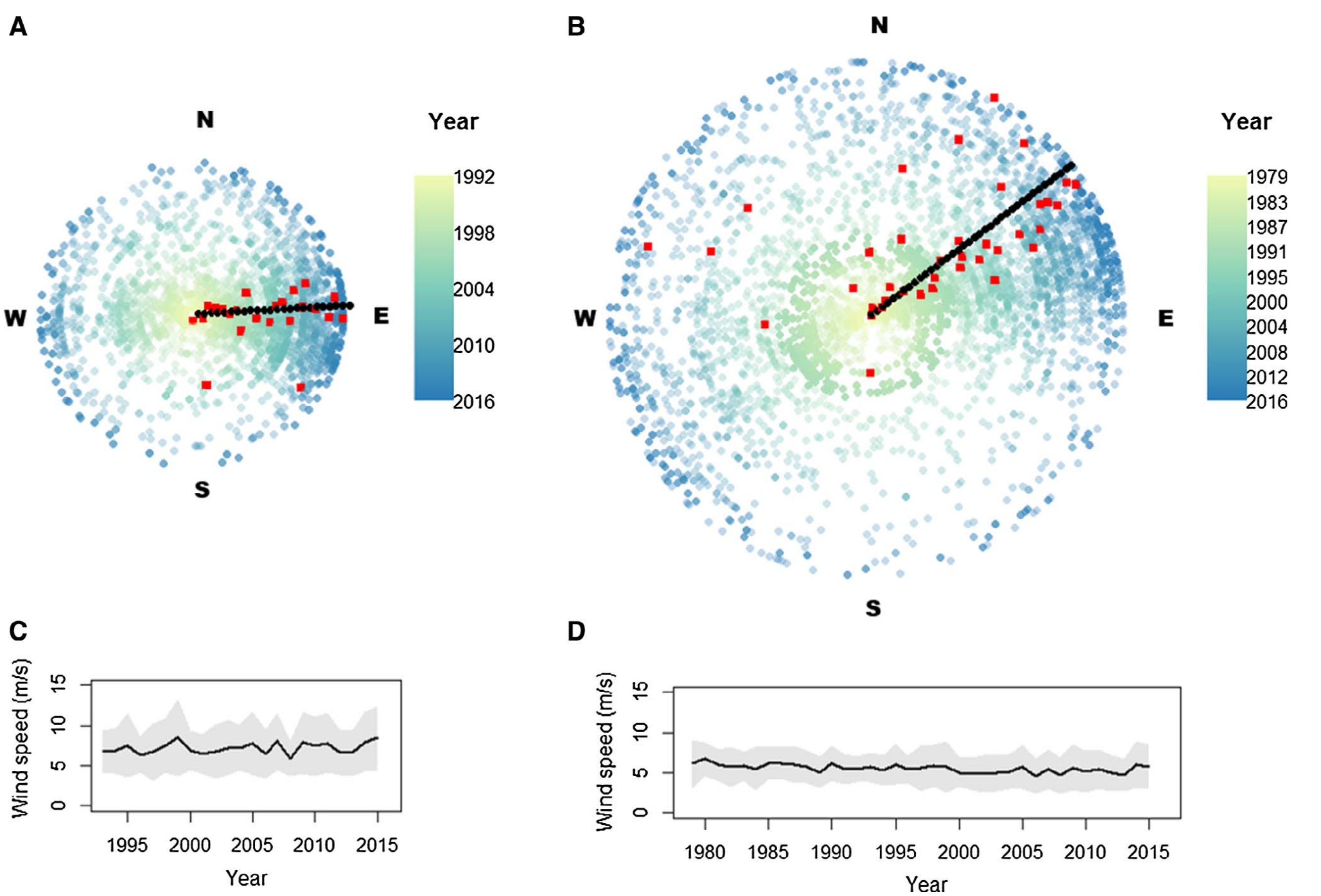

Fig. 4. Daily summer wind variables over time for West Dock (A,C) and Deadhorse Airport (B,D). The distributions of daily mean wind direction (A,B) show that winds tend to originate from the east. The earliest year of measurement is the most interior circle of points, the latest year is the most exterior. Semi-transparent points indicate daily average wind direction, colored by year. Opaque red squares indicate annual mean direction. Black line indicates overall mean direction for all years. Daily wind speeds (C,D) are shown as annual means ± SD (black line and grey shading). Wind speed varies between summers, but shows no long-term trends. (For interpretation of the references to colour in this figure legend, the reader is referred to the web version of this article.)

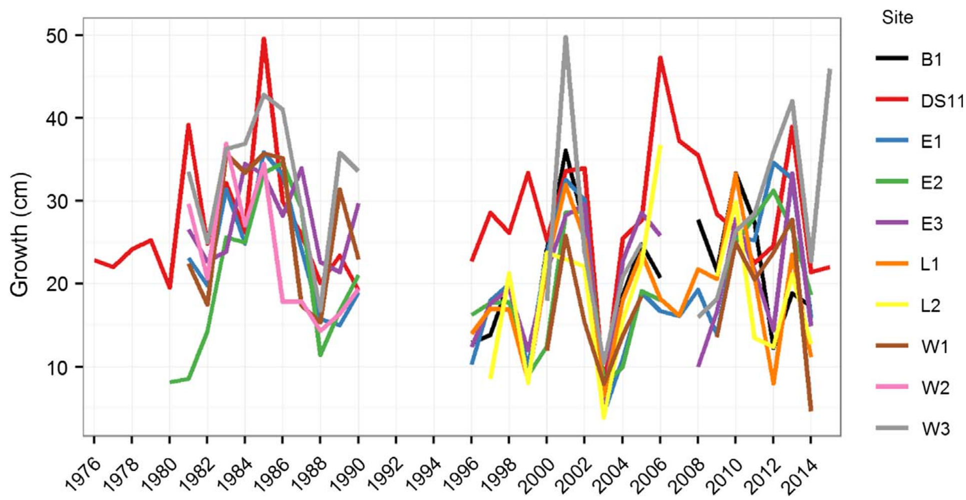

Fig. 5. Mean Laminaria solidungula growth (cm) varies between sites and years, with some years showing strong annual patterns (e.g. 2001 and 2003).

significantly affects MDI (linear regression, $p < 0.05$, $R^2 = 0.24$), TBI (linear regression, $p < 0.05$, $R^2 = 0.24$), and TH (linear regression, $p < 0.05$, $R^2 = 0.19$). This effect of wind is always negative. Plots of binned mean daily wind speed compared to percent surface irradiance for all ice-free dates at each site echo this negative relationship (Fig. 8). In contrast, there is no linear relationship between daily percent surface irradiance and sea ice concentration in the summer, with high irradiance values possible at high ice concentrations (Fig. 9). Although there is no relationship between mean wind direction and MDI, TBI, or TH for the 27 July – 31 August data, the proportion of westerly winds has a significant, negative effect on each of these irradiance variables (linear regressions, $p < 0.05$, $R^2_{MDI} = 0.21$, $R^2_{TBI} = 0.20$, $R^2_{TH} = 0.19$).

Modelled kelp production based on wind during the ice-free summer is more variable between sites than measured production, and shows a general increase over time in annual production (Fig. 10). Compared to measured production, the model is conservative, often underestimating annual kelp production, and has a high incidence of predicting zero production, especially for shallower sites.

4. Discussion

Although the ice-free season has lengthened over time in Stefansson Sound, we found no evidence of increased kelp production. Low light conditions prevail during the summer, suggesting that suspended sediments, often derived from wind-driven water motion, are integral in controlling light transmittance in shallow, nearshore regions of the Arctic. However, annual kelp production and long-term trends were not accurately predicted by our model, which relied on established relationships between wind speed and light attenuation during the ice-free summer. Instead, annual benthic light budgets – and therefore annual kelp production – appear to rely heavily on enhanced light transmittance in the days surrounding ice break-up. Overall, our results suggest that sea ice presence in these systems has a net positive effect on underwater light transmittance and marine primary production by attenuating swell and wave action.

Laminaria solidungula in Stefansson Sound survive at impressively low quantum budgets, reported previously by Dunton (1990) at 45 mol photons m^{-2} yr^{-1}, the lowest measured for any kelp population (Lüning and Dring, 1979 reported boreal *Laminaria hyperborea* at 71 mol photons m^{-2} yr^{-1}). In addition, *L. solidungula* exhibits saturation (E_k) and compensation (E_c) irradiance at 38 μmol photons m^{-2} sec^{-1} and 0.5–3 μmol photons m^{-2} sec^{-1}, respectively (Chapman and Lindley, 1980; Dunton and Jodwalis, 1988), among the lowest reported for marine macroalgae (Wiencke et al., 2006), and well below that of other cold water kelp species (*Laminaria digitata*: E_k and E_c = 150 μmol photons m^{-2} sec^{-1} and 6 μmol photons m^{-2} sec^{-1}, respectively; *Saccharina latissima*: E_k and E_c = 150 μmol photons m^{-2} sec^{-1} and 5 μmol photons m^{-2} sec^{-1}, respectively; *L. hyperborea* E_k and E_c = 90 μmol photons m^{-2} sec^{-1} and 9 μmol photons m^{-2} sec^{-1}, respectively; King and Schramm, 1976, Lüning, 1971). Consequently, because *L. solidungula* is very responsive to the low irradiance with an annual growth pattern strongly linked to summer open-water conditions (Dunton 1990), the species is an excellent indicator of interannual variations in the underwater light climate.

4.1. Ice concentration, wind dynamics, benthic irradiance, and kelp growth

Summer sea ice concentrations in Stefansson Sound have declined considerably since the 1980s (Fig. 2). Our analysis indicates that the open-water season (break-up end to freeze-up start) of the Boulder Patch area has gained approximately 17 days between 1979 and 2016 (Fig. 3). This rate of change is considerably less than that measured for the western coastal Beaufort Sea (~54 days over 34 years, Johnson and Eicken, 2016) and the Beaufort Sea as a whole (~36 days over 30 years, Markus et al., 2009; ~31 days over 34 years, Stroeve et al., 2014; ~41 days over 33 years Frey et al., 2015). However, the Beaufort Sea is a region characterized by considerable variability compared to other Arctic regions (Markus et al., 2009; Stroeve et al., 2014), and the rate of change for Stefansson Sound is similar to the trend for the entire Arctic (~20 days over 30 years, Markus et al., 2009; ~15 days over 34 years, Parkinson, 2014). While some of these differences may be attributed to varied definitions of "ice-covered", geomorphology is likely the main cause of disparity. Stefansson Sound is largely protected by a chain of barrier islands which affects the dynamics of landfast ice compared to pack ice. Landfast ice forms first in protected areas, such as lagoons and sheltered bays, and the timing of its freeze and melt are closely tied to the onset of freezing and thawing temperatures, respectively (Barry et al., 1979; Mahoney et al., 2014). As a result, ice presence in sheltered coastal waters such as Stefansson Sound may respond to different forcing and exhibit more moderate long-term trends than in exposed and offshore waters.

One expected outcome of decreased seasonal ice is an increase in underwater light and annual production in *L. solidungula* over time (i.e. Krause-Jensen et al., 2012; Clark et al., 2013), as demonstrated by our productivity model (Fig. 10). Our data, however, do not show such a trend (Figs. 4 and 10). Previous research has demonstrated that while there is a strong correlation between annual benthic irradiance and *L. solidungula* production, there is no correlation between daily surface and underwater irradiance in Stefansson Sound (Dunton, 1990). Additionally, the timing of ice dynamics has no direct impact on annual

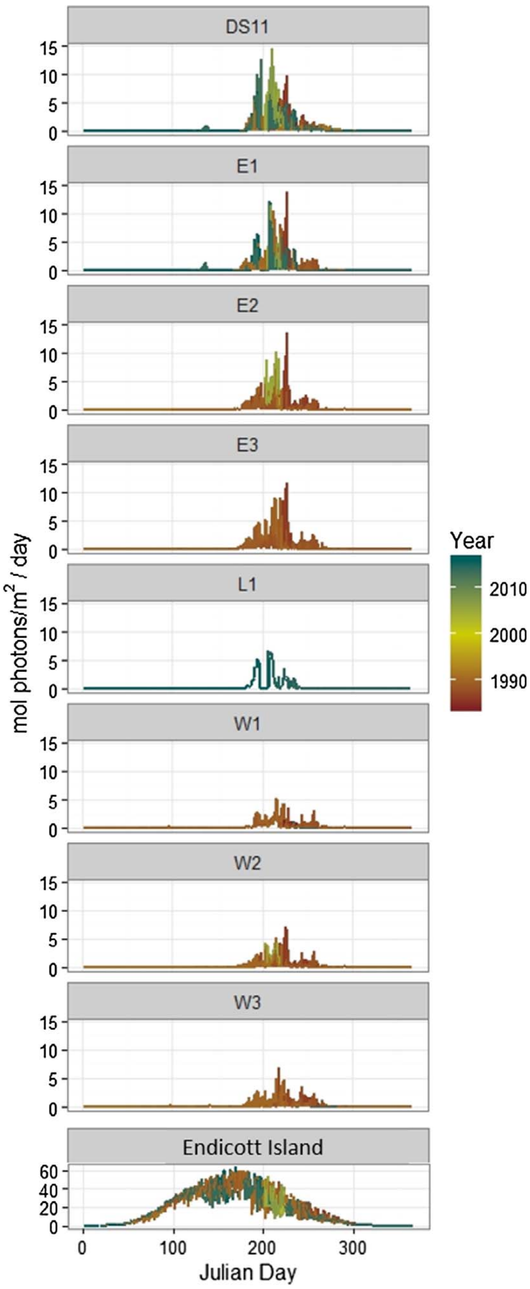

Fig. 6. Seasonal pattern of both incident (Endicott Island) and underwater irradiance (mol photons m^{-2} day^{-1}) on the seabed at eight locations in Stefansson Sound by year. Note change in scale for surface irradiance.

kelp production. Instead, annual benthic light budgets in Stefansson Sound are primarily limited by resuspension of sediments by wind-induced water motion (Aumack et al., 2007). This is partially demonstrated by the considerable accumulation of H_{sat} during the dates surrounding ice break-up (Fig. 7), when wind-driven water motion is limited by high sea ice concentrations. The negative relationship between wind speed and benthic irradiance over month-long periods, and the prevalence of low light conditions during the ice-free season (Table 1), further emphasize the link between wind and light attenuation.

The lack of a significant relationship between ice concentration and benthic light during late July through August indicates that the negative effects of wind outweigh the potentially remediating effects of any sea ice that lingers in the nearshore area after the open-water season is underway. As in other shallow aquatic systems, rates of particle settlement and transport of suspended sediments confound the connection between benthic irradiance and wind (Van Duin et al., 2001). The effect of wind direction on the entrainment or advection of turbid coastal waters adds additional complexity to this relationship. It appears that the frequency of short-term increases in underwater light transmittance, under favorable wind and ice conditions ultimately determine the annual benthic light budget in this system.

The temporal accumulation of H_{sat} suggests that the days surrounding ice break-up contribute significantly (as much as 75–100%; Fig. 7) to annual benthic light budgets and annual kelp production. Underwater irradiance during this time depends on the amount of sediments contained within the ice (Dunton et al., 1982; Kempema et al., 1989), as well as ice dynamics during break-up, which are difficult to predict, and therefore not included in our production model. The omission of the break-up period may explain why the ice- and wind-based production model often underestimated kelp growth (Fig. 10). The drastically reduced light levels during the ice-free summer and the lack of relationship to annual kelp growth demonstrate that light conditions during the ice-free summer are usually poor. Consequently, contracted sea ice extent may simply contribute to wind-driven mixing of the water column and increased suspended sediments earlier in the year, effectively diminishing benthic irradiance and kelp production during the ice-free summer.

Reduced sea ice coverage in the coastal Beaufort Sea has increased wave fetch and intensified wave energy (Thomson and Rogers, 2014; Thomson et al., 2016) that can substantially increase suspended sediments (Trefry et al., 2009). Other studies in this region show that wave height is related to wind speed, as well as ice concentration (Manson and Solomon, 2007). Therefore the strengthening of easterly winds in the region since the mid-2000 s may also contribute to enhanced sediment resuspension (Wood et al., 2013, 2015), though this trend was not reflected in the wind measurements recorded at the Prudhoe Bay weather stations.

Current projections for macrophyte communities in Arctic marine systems assume that benthic irradiance will increase as sea ice extent contracts (i.e. Clark et al., 2013, Krause-Jensen and Duarte, 2014). The long-term data presented here show that this assumption may not apply to inner shelf regions, especially marginal Arctic seas that receive substantial river inputs during the summer open-water period. This also agrees with results from a glacially-influenced site, where sediment-laden glacial meltwater is thought to have shrank the euphotic zone over time (Bartsch et al., 2016). Light attenuation by suspended sediments demonstrably affects irradiance available for primary production, both in the water column (Van Duin et al., 2001) and in the benthos (Anthony et al., 2004; Aumack et al., 2007), and should be considered for Arctic ecosystem change scenarios.

4.2. The Arctic inner shelf under future climate change

Shallow inner shelf zones make up 20% of the area of Arctic shelves (Fritz et al., 2017). Outside of Greenland and the Canadian Archipelago, these systems experience considerable inputs from Arctic rivers during the melt season that contribute to total suspended sediment (TSS) concentrations (Gordeev et al., 1996; Holmes et al., 2002; Gordeev, 2006; McClelland et al., 2011). Coastal erosion also significantly contributes to elevated TSS levels in inner shelf zones (Reimnitz et al., 1988; Hill and Nadeau, 1989), which are often maintained by wind events that resuspend unconsolidated sediments on shallow shelves (Hill and Nadeau, 1989). The reduction in water transparency in response to increased TSS, which is accentuated by expanded fetch and diminished ice extent, demonstrates the effects of a warming Arctic on primary production, especially on the coast and inner shelf. Consequently, we should expect that coastal ecosystems will respond differently to climate change than deeper, offshore seasonal ice zones.

As warming continues, multiple environmental factors in nearshore Arctic areas will cause average summer light attenuation to surpass

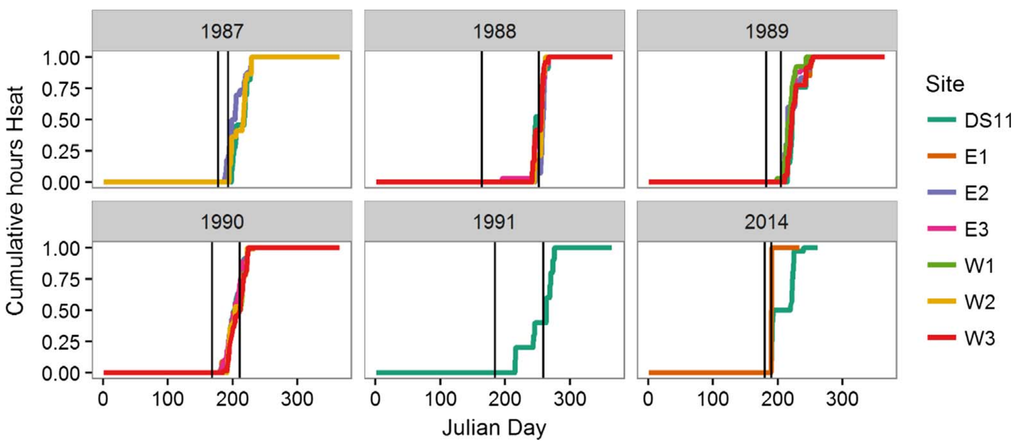

Fig. 7. Cumulative H_{sat}, as proportion of annual H_{sat}, illustrates the rapid accumulation of hours of saturating irradiance during and directly following the period of ice break-up, based on available *in situ* irradiance data from each site from July through September. Pairs of black vertical lines frame the period between start of break-up and when sea ice concentration reaches 15%.

Table 1
Summary of underwater daily light values for ice-free summer (end of break-up to the start of freeze-up). Differences in mean daily surface irradiance between sites are due to differences in benthic light data coverage over time (Supp. Table 1).

Site	Depth (m)	Mean daily surface irradiance (mol photons m^{-2} day^{-1}))	Mean daily percent surface irradiance ± SD	Mean light attenuation, k (m^{-1})	Percent of days with benthic photon flux of 0	Mean daily hours H_{sat}	Percent of days with 0 h H_{sat}
DS11	6.1	15.5	4.1 ± 6.2	0.52	20.9	1.9 ± 4.0	77.8
E1	4.4	15.1	3.2 ± 6.4	0.78	29.9	1.7 ± 4.0	81.5
E2	4.3	13.8	3.1 ± 6.2	0.81	38.1	1.5 ± 3.6	82.8
E3	5.5	12.7	3.6 ± 6.6	0.60	35.4	1.7 ± 3.9	78.8
L1	5.5	17.0	1.9 ± 3.8	0.72	35.3	1.4 ± 3.7	82.7
W1	6.0	12.5	1.9 ± 3.7	0.66	39.3	0.8 ± 2.5	87.0
W2	6.2	13.3	2.2 ± 4.2	0.62	41.2	0.9 ± 2.9	87.9
W3	6.6	12.2	2.3 ± 4.3	0.57	43.9	1.1 ± 2.8	84.2

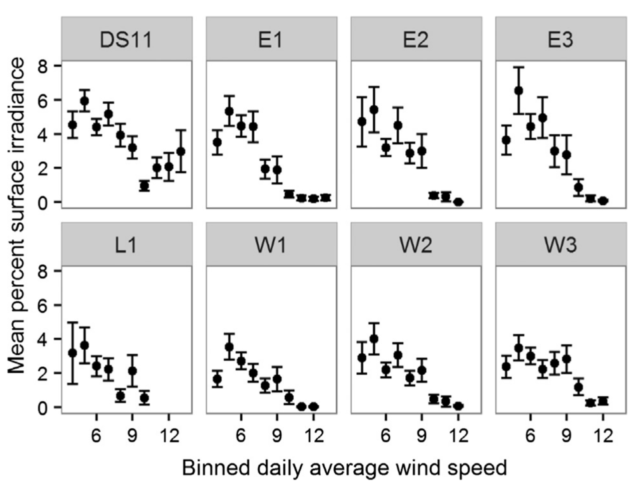

Fig. 8. Mean daily underwater irradiance, as percent surface irradiance, at each site in relation to coastal wind speed calculated from the Deadhorse Airport station (Eq. (1)).

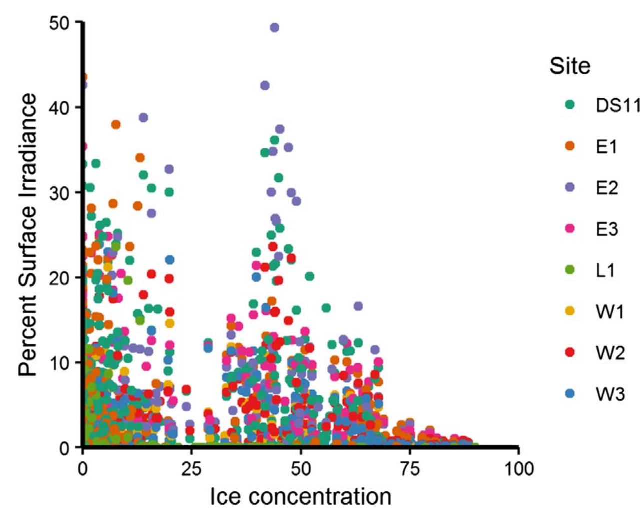

Fig. 9. Distribution of daily underwater irradiance values (as percent of surface irradiance) as a function of ice concentration during the period from the start of ice break-up to the start of freeze-up. Note that high irradiance values are possible at relatively high ice concentrations.

current levels (~0.8 m^{-1}; Table 1). The persistence of these high attenuation conditions, which match the turbid conditions previously measured in Stefansson Sound (Dunton, 1990; Dunton et al., 2009), will alter regimes of underwater light transmittance and primary productivity (Fig. 11). First, the reduction of sea ice will increase the incident sunlight to the ocean, leading to enhanced capacity for primary productivity at the surface. However, this reduction in sea ice will also lead to lengthened fetch, larger swell, stronger wave activity in the nearshore, and higher incidence of sediment resuspension (Wegner et al., 2003; Walker et al., 2008; Thomson and Rogers, 2014; Thomson et al., 2016). Nearshore wave activity also intensifies coastal erosion, aided by melting permafrost and sea level rise (ACIA, 2005, Overeem et al., 2011). Currently, both sheltered mainland-lagoon and open-ocean exposed coastlines of the Beaufort Sea are eroding at rates of 0.9–1.8 m y^{-1}, respectively (Gibbs and Richmond, 2015). Globally, rates have been measured as high as 25 m y^{-1} (Jones et al., 2009; Gunther et al., 2015). Beaufort Sea Coast erosion rates appear to have increased, or even doubled over the past five decades (Jones et al., 2008, 2009). As the climate continues to warm, most Arctic coastlines are expected to experience accelerated coastal erosion (Fritz et al., 2017, ACIA, 2005). River discharge to the Arctic Ocean is also increasing, with measured increase of ~11% from 1964 to 2000 (McClelland et al., 2006). This will contribute to intensified fluvial

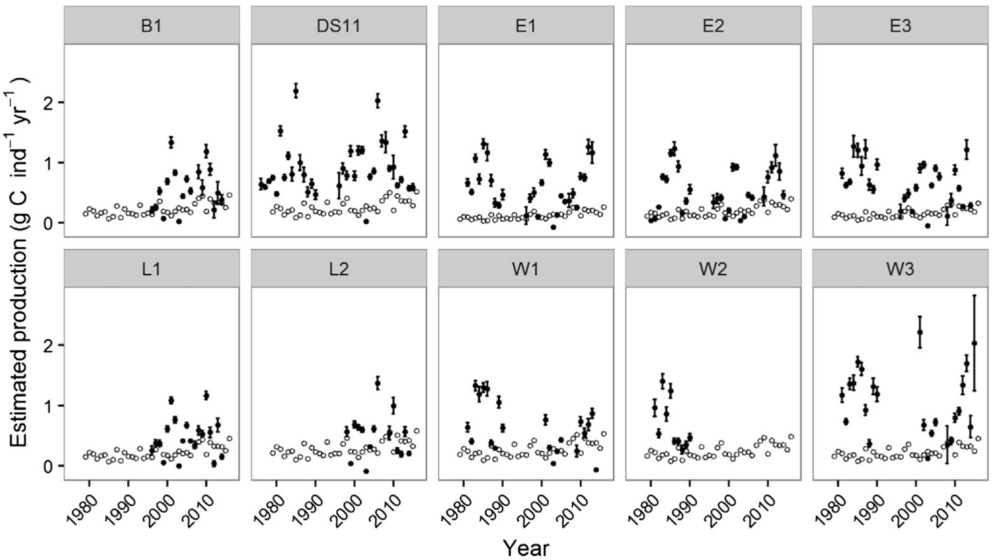

Fig. 10. Modelled kelp production (white circles), calculated for an average-sized individual (22.5 cm basal blade length) based on the relationship between wind velocity, total suspended solids, and light attenuation during the ice-free period, compared to measured mean kelp production (black circles ± SE) calculated from blade elongation.

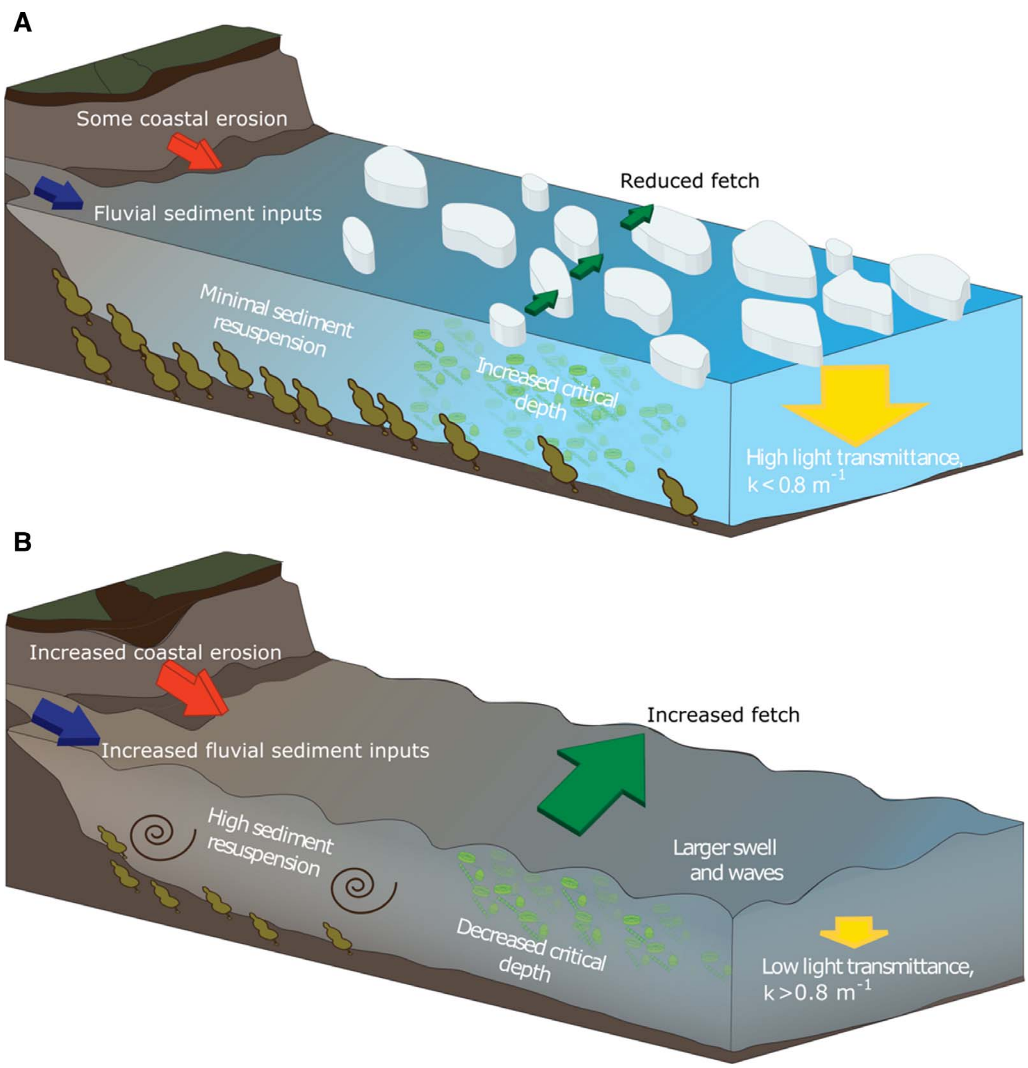

Fig. 11. Conceptual diagram of the effects of (a) summer ice cover versus (b) reduced summer ice cover on processes affecting the underwater light environment in shallow inshore (< 10 m) Arctic ecosystems. Reduced ice will increase coastal erosion, lead to larger swell, and increase sediment resuspension, which will combine with enhanced fluvial sediment inputs to ultimately increase light attenuation (k). This will decrease annual growth of benthic macrophytes, and shift depth distributions of pelagic and benthic primary producers by shallowing the critical depth.

sediment flux, estimated to rise by 30–122% for the six largest Arctic rivers by the end of the century (Gordeev, 2006).

The additive effects of sea ice loss, coastal erosion, and enhanced fluvial inputs will ultimately increase suspended sediments in Arctic inner shelf waters during the open-water season (Fig. 11). Our research suggests that as summer ice concentrations continue to decrease, the annual benthic light budget in nearshore areas will progressively depend on light transmitted through the ice and water before and during break-up. It also shows that primary production may shift in unexpected ways in the future, depending on local characteristics. In areas with high suspended sediments, benthic production may not be enhanced by ice loss, but will increasingly rely on light transmittance during break-up. Phytoplankton productivity in the nearshore Arctic will also depend on the balance between light attenuation by suspended sediments and nutrient concentrations in the upper water column, which are similarly determined by sediment resuspension, erosion, and fluvial inputs. Decreased light transmission during summer will shallow the critical depth of growth, altering depth distributions of benthic and planktonic primary producers. Our work demonstrates that environmental factors that characterize Arctic inner shelves, particularly suspended sediments, should be considered in projections that evaluate the response of Arctic ecosystems to climate change.

Acknowledgments

We thank all the individuals who have contributed towards the success of our work in the Boulder Patch over the last four decades. These include C. Aumack, G. Boland, P. Bucolo, G. Cinkovich, D. Funk, J. Hanes, K. Iken, B. Konar, L. Martin, J. Olson, P. Plesha, D. Pope, S. Schonberg, and G. F. Smith for valuable field and diving assistance. We especially thank J. Dunton and T. Dunton for their inimitable logistical expertise. Early drafts of this manuscript were greatly improved by comments from A. Muth with statistical advice provided by L. Scheef. Several awards to KHD have supported the field research associated with the Boulder Patch starting with the Outer Continental Shelf Environmental Assessment Program (OCSEAP) in 1978, the National Science Foundation, BP Exploration, Inc., Hilcorp, and a sequence of awards from the Bureau of Ocean Energy Management (BOEM). A special note of thanks to the very special team of workers at the Endicott Production facility, whom have provided their friendship, help, and advice over three decades. This long-term study would never had been possible without the exceptional vision of D. Prentki and C. Coon, our successive BOEM Contracting Office Representatives, who have been unwavering in their support over the past decade. This synthesis was funded under BOEM Award Number M12AS00001 as part of the Continuation of the Arctic Nearshore Impact Monitoring in Development Area (cANIMIDA) Project and the BOEM Alaska Environmental Studies Program.

Appendix A. Supplementary material

Supplementary data associated with this article can be found, in the online version, at http://dx.doi.org/10.1016/j.pocean.2018.02.016.

References

ACIA, 2005. Arctic Climate Impact Assessment. Cambridge University Press, 1042p.

Agostinelli, C., Lund, U. 2017. R package 'circular': Circular Statistics (version 0.4-93). <https://r-forge.r-project.org/projects/circular/>.

Anthony, K.R.N., Ridd, P.V., Orpin, A.R., Larcombe, P., Lough, J., Connolly, S., Anthony, D., 2004. Temporal variation of light availability in coastal benthic habitats: effects of clouds, turbidity, and tides. Limnol. Oceanogr. 49, 2201–2211. http://dx.doi.org/10.4319/lo.2004.49.6.2201.

Aumack, C.F., Dunton, K.H., Burd, A.B., Funk, D.W., Maffione, R.A., 2007. Linking light attenuation and suspended sediment loading to benthic productivity within an Arctic kelp-bed community 1. J. Phycol. 43, 853–863. http://dx.doi.org/10.1111/j.1529-8817.2007.00383.x.

Aumack, Craig F., 2003. Linking water turbidity and TSS loading to kelp productivity within the Stefansson Sound Boulder Patch. MS Thesis.

Barnes, P.W., Reimnitz, E., 1974. Sedimentary processes on arctic shelves off the northern coast of Alaska. In: Reed, J.C., Sater, J.E. (Eds.), The Coast and Shelf of the Beaufort Sea. Arctic Institute of North America, Arlington, VA, pp. 439–476.

Barry, R.G., Moritz, R.E., Rogers, J.C., 1979. The fast ice regimes of the Beaufort and Chukchi Sea coasts. Alaska. Cold Reg. Sci. Technol. 1, 129–152. http://dx.doi.org/10.1016/0165-232X(79)90006-5.

Bartsch, I., Paar, M., Fredriksen, S., Schwanitz, M., Daniel, C., Hop, H., Wiencke, C., 2016. Changes in kelp forest biomass and depth distribution in Kongsfjorden, Svalbard, between 1996–1998 and 2012–2014 reflect Arctic warming. Polar Biol. 39, 2021–2036. http://dx.doi.org/10.1007/s00300-015-1870-1.

Chamberlain, S., 2016. rnoaa: 'NOAA' Weather Data from R R package version 6 2016 5 < >.

Chapman, A., Lindley, J., 1980. Seasonal growth of Laminaria solidungula in the Canadian High Arctic in relation to irradiance and dissolved nutrient concentrations. Mar. Biol. 5, 1–5. http://dx.doi.org/10.1007/BF00420961.

Clark, G.F., Stark, J.S., Johnston, E.L., Runcie, J.W., Goldsworthy, P.M., Raymond, B., Riddle, M.J., 2013. Light-driven tipping points in polar ecosystems. Glob. Chang. Biol. 19, 3749–3761. http://dx.doi.org/10.1111/gcb.12337.

Dunton, K.H., 1984. An annual carbon budget for an arctic kelp community. In: Barnes, P.W., Schell, D.M., Reimnitz, E. (Eds.), The Alaskan Beaufort Sea: ecosystems and environments. Academic Press, Orlando, FL, pp. 311–326.

Dunton, K.H., 1985. Growth of Dark-exposed Laminaria saccharina (L.) Lamour. and Laminaria solidungula J. Ag. (Laminariales : Phaeophyta) in the Alaskan Beaufort Sea. J. Exp. Mar. Bio. Ecol. 94, 181–189. http://dx.doi.org/10.1016/0022-0981(85)90057-7.

Dunton, K.H., 1990. Growth and production in Laminaria solidungula: relation to continuous underwater light levels in the Alaskan High Arctic. Mar. Biol. 106, 297–304. http://dx.doi.org/10.1007/BF01314813.

Dunton, K.H., Schonberg, S.V., Funk, D.W., 2009. Interannual and spatial variability in light attenuation: evidence from three decades of growth in the arctic kelp, Laminaria solidungula, p. 271–284. In: Smithsonian at the Poles/Contributions to International Polar Year Science.

Dunton, K.H., Jodwalis, C.M., 1988. Photosynthetic performance of Laminaria solidungula measured in situ in the Alaskan High Arctic. Mar. Biol. 98, 277–285. http://dx.doi.org/10.1007/BF00391206.

Dunton, K.H., Reimnitz, E.R.K., Schonberg, S., 1982. An Arctic Kelp Community in the Alaskan Beaufort Sea. Arctic 35, 465–484. http://dx.doi.org/10.14430/arctic2355.

Dunton, K., Schell, D., 1986. Seasonal carbon budget and growth of Laminaria solidungula in the Alaskan High Arctic. Mar. Ecol. Prog. Ser. 31, 57–66. http://dx.doi.org/10.3354/meps031057.

Dunton, K.H., Schell, D.M., 1987. Dependence of consumers on macroalgal (Laminaria solidungula) carbon in an arctic kelp community: d 13 C evidence. Mar. Biol. 93, 615–625.

Dunton, K.H., Schonberg, S.V., Martin, L.R., Mueller, G.S., 1992. Seasonal and Annual Variations in the underwater light environment of an Arctic kelp community. Diving Sci. 83–92.

Frey, K.E., Moore, G.W.K., Cooper, L.W., Grebmeier, J.M., 2015. Divergent patterns of recent sea ice cover across the Bering, Chukchi, and Beaufort seas of the Pacific Arctic Region. Prog. Oceanogr. 136, 32–49. http://dx.doi.org/10.1016/j.pocean.2015.05.009.

Fritz, M., Vonk, J.E., Lantuit, H., 2017. Collapsing Arctic coastlines. Nat. Clim. Change 7, 6–7. http://dx.doi.org/10.1038/nclimate3188.

Gibbs, A.E., Richmond, B.M., 2015. National assessment of shoreline change—Historical shoreline change along the north coast of Alaska, U.S.–Canadian border to Icy Cape: U.S. Geological Survey Open-File Report 2015–1048.

Glud, R.N., Woelfel, J., Karsten, U., Kühl, M., Rysgaard, S., 2009. Benthic microalgal production in the Arctic: applied methods and status of the current database. Bot. Mar. 52, 559–571. http://dx.doi.org/10.1515/BOT.2009.074.

Gordeev, V.V., 2006. Fluvial sediment flux to the Arctic Ocean. Geomorphology 80, 94–104. http://dx.doi.org/10.1016/j.geomorph.2005.09.008.

Gordeev, V.V., Martin, J.M., Sidorov, I.S., Sidorova, M.V., 1996. A reassessment of the Eurasian river input of water, sediment, major elements, and nutrients to the Arctic Ocean. Am. J. Sci. 296, 664–691. http://dx.doi.org/10.2475/ajs.296.6.664.

Gunther, F., Overduin, P.P., Yakshina, I.A., Opel, T., Baranskaya, A.V., Grigoriev, M.N., 2015. Observing Muostakh disappear: permafrost thaw subsidence and erosion of a ground-ice-rich island in response to arctic summer warming and sea ice reduction. Cryosphere 9, 151–178. http://dx.doi.org/10.5194/tc-9-151-2015.

Henley, W., Dunton, K., 1995. A seasonal comparison of carbon, nitrogen, and pigment content in Laminaria solidungula and L. saccharina (Phaeophyta) in the Alaskan Arctic. J. Phycol. 331, 325–331. http://dx.doi.org/10.1111/j.0022-3646.1995.00325.x.

Hill, P.R., Nadeau, O.C., 1989. Storm-dominated Sedimentation on the Inner Shelf of the Canadian Beaufort Sea. J. Sediment. Petrol. 59, 455–468. http://dx.doi.org/10.1306/212F8FC1-2B24-11D7-8648000102C1865D.

Holmes, R.M., McClelland, J.W., Peterson, B.J., Shiklomanov, I.A., Shiklomanov, A.I., Zhulidov, A.V., Gordeev, V.V., Bobrovitskaya, N.N., 2002. A circumpolar perspective on fluvial sediment flux to the Arctic ocean. Glob. Biogeochem. Cycles 16, 14–45. http://dx.doi.org/10.1029/2001GB001849.

Ji, R., Jin, M., Varpe, Ø., 2013. Sea ice phenology and timing of primary production pulses in the Arctic Ocean. Glob. Chang. Biol. 19, 734–741. http://dx.doi.org/10.1111/gcb.12074.

Johnson, M., Eicken, H., 2016. Estimating Arctic sea-ice freeze-up and break-up from the satellite record: a comparison of different approaches in the Chukchi and Beaufort Seas. Elem. Sci. Anthr. 4, 124. http://dx.doi.org/10.12952/journal.elementa.000124.

Jones, B.M., Hinkel, K.M., Arp, C.D., Eisner, W.R., 2008. Modern erosion rates and loss of coastal features and sites, Beaufort Sea coastline, Alaska. Arctic 61, 361–372.

Jones, B.M., Arp, C.D., Jorgenson, M.T., Hinkel, K.M., Schmutz, J.A., Flint, P.L., 2009. Increase in the rate and uniformity of coastline erosion in Arctic Alaska. Geophys. Res. Lett. 36, 1–5. http://dx.doi.org/10.1029/2008GL036205.

Kahru, M., Brotas, V., Manzano-Sarabia, M., Mitchell, B.G., 2011. Are phytoplankton blooms occurring earlier in the Arctic? Glob. Chang. Biol. 17, 1733–1739. http://dx.doi.org/10.1111/j.1365-2486.2010.02312.x.

Kempema, E.W., Reimnitz, E., Barnes, P.W., 1989. Sea ice sediment entrainment and rafting in the Arctic. J. Sediment. Petrol. 59, 308–317. http://dx.doi.org/10.1306/212F8F80-2B24-11D7-8648000102C1865D.

King, R.J., Schramm, W., 1976. Photosynthetic rates of benthic marine algae in relation to light intensity and seasonal variations. Mar. Biol. 37, 215–222. http://dx.doi.org/10.1007/BF00387606.

Krause-Jensen, D., Duarte, C.M., 2014. Expansion of vegetated coastal ecosystems in the future Arctic. Front. Mar. Sci. 1, 1–10. http://dx.doi.org/10.3389/fmars.2014.00077.

Krause-Jensen, D., Marbà, N., Olesen, B., et al., 2012. Seasonal sea ice cover as principal driver of spatial and temporal variation in depth extension and annual production of kelp in Greenland. Glob. Change Biol. 18, 2981–2994. http://dx.doi.org/10.1111/j.1365-2486.2012.02765.x.

Krause-Jensen, D., Marbà, N., Sanz-Martin, M., Hendriks, I.E., Thyrring, J., Carstensen, J., Sejr, M.K., Duarte, C.M., 2016. Long photoperiods sustain high pH in Arctic kelp forests. Sci. Adv. 2, e1501938. http://dx.doi.org/10.1126/sciadv.1501938.

Lüning, K., Dring, M.J., 1979. Continuous underwater light measurement near Helgoland (North Sea) and its significance for characteristic light limits in the sublittoral region. Helgolander Wiss. Meeresunters 32, 403–424. http://dx.doi.org/10.1007/BF02277985.

Lüning, K., 1971. Seasonal growth of Laminaria hyperborean under recorded underwater light conditions near Helgoland. In: Crisp, D.J. (ed.), Proceedings of the 4th European Marine Biology Symposium. University Press, Cambridge, pp. 347–361.

Mahoney, A.R., Eicken, H., Gaylord, A.G., Gens, R., 2014. Landfast sea ice extent in the Chukchi and Beaufort Seas: the annual cycle and decadal variability. Cold Reg. Sci. Technol. 103, 41–56. http://dx.doi.org/10.1016/j.coldregions.2014.03.003.

Manson, G.K., Solomon, S.M., 2007. Past and future forcing of Beaufort Sea coastal change. Atmos.-Ocean 45, 107–122. http://dx.doi.org/10.3137/ao.450204.

Markus, T., Stroeve, J.C., Miller, J., 2009. Recent changes in Arctic sea ice melt onset, freezeup, and melt season length. J. Geophys. Res. Ocean. 114, 1–14. http://dx.doi.org/10.1029/2009JC005436.

McClelland, J.W., Déry, S.J., Peterson, B.J., Holmes, R.M., Wood, E.F., 2006. A pan-arctic evaluation of changes in river discharge during the latter half of the 20th century. Geophys. Res. Lett. 33, 2–5. http://dx.doi.org/10.1029/2006GL025753.

McClelland, J.W., Holmes, R.M., Dunton, K.H., Macdonald, R.W., 2011. The Arctic ocean estuary. Estuaries Coasts 35, 353–368. http://dx.doi.org/10.1007/s12237-010-9357-3.

McMeans, B.C., McCann, K.S., Humphries, M., Rooney, N., Fisk, A.T., 2015. Food web structure in temporally-forced ecosystems. Trends Ecol. Evol. 30, 662–672. http://dx.doi.org/10.1016/j.tree.2015.09.001.

O'Brien, M.C., Macdonald, R.W., Melling, H., Iseki, K., 2006. Particle fluxes and geochemistry on the Canadian Beaufort Shelf: implications for sediment transport and deposition. Cont. Shelf Res. 26, 41–81. http://dx.doi.org/10.1016/j.csr.2005.09.007.

Overeem, I., Anderson, R.S., Wobus, C.W., Clow, G.D., Urban, F.E., Matell, N., 2011. Sea ice loss enhances wave action at the Arctic coast. Geophys. Res. Lett. 38, 1–6. http://dx.doi.org/10.1029/2011GL048681.

Parkinson, C.L., 2014. Spatially mapped reductions in the length of the Arctic sea ice season. Geophys. Res. Lett. 41, 4316–4322. http://dx.doi.org/10.1002/2014GL060434.

Post, E., Bhatt, U.S., Bitz, C.M., et al., 2013. Ecological consequences of sea-ice decline. Science 341, 519–524. http://dx.doi.org/10.1126/science.1235225.

R Core Team R: A language and environment for statistical computing 2016 R Foundation for Statistical Computing Vienna, Austria < https://www.R-project.org/ >.

Reimnitz, E., Graves, S.M., Barnes, P.W., 1988. Beaufort Sea coastal erosion, shoreline evolution, and sediment flux. US Department of the Interior, Geological Survey.

Rember, R.D., Trefry, J.H., 2004. Increased concentrations of dissolved trace metals and organic carbon during snowmelt in rivers of the alaskan arctic. Geochim. Cosmochim. Acta 68, 477–489. http://dx.doi.org/10.1016/S0016-7037(03)00458-7.

Renaud, P.E., Løkken, T.S., Jørgensen, L.L., Berge, J., Johnson, B.J., 2015. Macroalgal detritus and food-web subsidies along an Arctic fjord depth-gradient. Front. Mar. Sci. 2, 1–15. http://dx.doi.org/10.3389/fmars.2015.00031.

Serreze, M.C., Stroeve, J.C., 2015. Arctic sea ice trends, variability and implications for seasonal ice forecasting. Philos. Trans. R. Soc. A Math. Phys Eng. Sci. 373, 20140159. http://dx.doi.org/10.1098/rsta.2014.0159.

Stroeve, J.C., Markus, T., Boisvert, L., Miller, J., Barrett, A., 2014. Changes in Arctic melt season and implifications for sea ice loss. Geophys. Res. Lett. 41, 1216–1225. http://dx.doi.org/10.1002/2013GL058951.

Thomson, J., Rogers, W.E., 2014. Swell and sea in the emerging Arctic Ocean. Geophys. Res. Lett. 41, 3136–3140. http://dx.doi.org/10.1002/2014GL059983.

Thomson, J., Fan, Y., Stammerjohn, S., et al., 2016. Emerging trends in the sea state of the Beaufort and Chukchi seas. Ocean Model. 105, 1–12. http://dx.doi.org/10.1016/j.ocemod.2016.02.009.

Trefry, J. H., Trocine, R.P., Alkire, M.B., Semmler, C.M., Savoie, M., Rembe, R.D., 2009. cANIMIDA Tasks 3 and 4: Sources, Concentrations, Composition, Partitioning and Dispersion Pathways for Suspended Sediments and Potential Metal Contaminants in the Coastal Beaufort Sea. USDOI, MMS, Alaska OCS Region, Anchorage, AK. OCS Study.

Van Duin, E.H.S., Blom, G., Los, F.J., et al., 2001. Modeling underwater light climate in relation to sedimentation, resuspension, water quality and autotrophic growth. Hydrobiologia 444, 25–42. http://dx.doi.org/10.1023/A:1017512614680.

Walker, T.R., Grant, J., Cranford, P., Lintern, D.G., Hill, P., Jarvis, P., Barrell, J., Nozais, C., 2008. Suspended sediment and erosion dynamics in Kugmallit Bay and Beaufort Sea during ice-free conditions. J. Mar. Syst. 74, 794–809. http://dx.doi.org/10.1016/j.jmarsys.2008.01.006.

Wassmann, P., Duarte, C.M., Agustí, S., Sejr, M.K., 2011. Footprints of climate change in the Arctic marine ecosystem. Glob. Chang. Biol. 17, 1235–1249. http://dx.doi.org/10.1111/j.1365-2486.2010.02311.x.

Wassmann, P., Reigstad, M., 2011. Future Arctic ocean seasonal ice zones and implications for pelagic-benthic coupling. Oceanography 24, 220–231. http://dx.doi.org/10.5670/oceanog.2011.74.

Wegner, C., Hölemann, J.A., Dmitrenko, I., Kirillov, S., Tuschling, K., Abramova, E., Kassens, H., 2003. Suspended particulate matter on the Laptev Sea shelf (Siberian Arctic) during ice-free conditions. Estuar. Coast. Shelf Sci. 57, 55–64. http://dx.doi.org/10.1016/S0272-7714(02)00328-1.

Wiencke, C., Clayton, M.N., Gómez, I., et al., 2006. Life strategy, ecophysiology and ecology of seaweeds in polar waters. Rev. Environ. Sci. Bio/Technology 6, 95–126. http://dx.doi.org/10.1007/s11157-006-9106-z.

Wood, K.R., Overland, J.E., Salo, S.a., Bond, N.a., Williams, W.J., Dong, X., 2013. Is there a "new normal" climate in the Beaufort Sea? Polar Res. 32, 1–9. http://dx.doi.org/10.3402/polar.v32i0.19552.

Wood, K.R., Bond, N.A., Danielson, S.L., Overland, J.E., Salo, S.A., Stabeno, P.J., Whitefield, J., 2015. A decade of environmental change in the Pacific Arctic region. Prog. Oceanogr. 136, 12–31. http://dx.doi.org/10.1016/j.pocean.2015.05.005.